



Contents lists available at ScienceDirect

Journal of Hazardous Materials

journal homepage: [www.elsevier.com/locate/jhazmat](http://www.elsevier.com/locate/jhazmat)

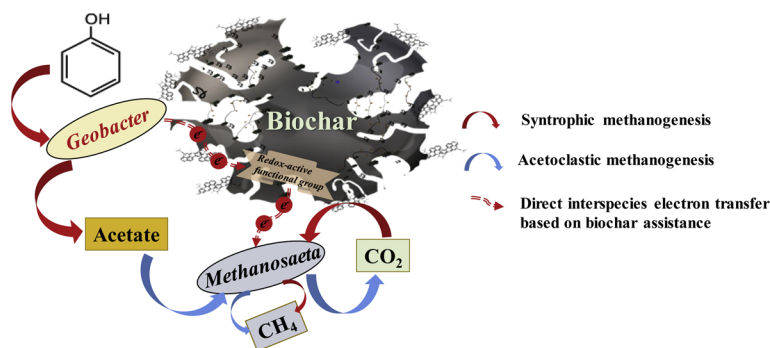
## Redox-based electron exchange capacity of biowaste-derived biochar accelerates syntrophic phenol oxidation for methanogenesis via direct interspecies electron transfer

Gaojun Wang<sup>a,1</sup>, Xin Gao<sup>a,1</sup>, Qian Li<sup>a,\*</sup>, Hexiang Zhao<sup>b</sup>, Yanzheng Liu<sup>a</sup>, Xiaochang C. Wang<sup>a</sup>, Rong Chen<sup>a,\*</sup>

<sup>a</sup> International Science and Technology Cooperation Center for Urban Alternative Water Resources Development, Key Laboratory of Northwest Water Resource, Environment and Ecology, MOE, Engineering Technology Research Center for Wastewater Treatment and Reuse, Shaanxi, Key Laboratory of Environmental Engineering, Shaanxi, Xi'an University of Architecture and Technology, No. 13 Yanta Road, Xi'an 710055, PR China

<sup>b</sup> Shaanxi Coal and Chemistry Technology Institute Co., Ltd., Xi'an 710065, PR China

### GRAPHICAL ABSTRACT



### ARTICLE INFO

Editor: L. Eder

#### Keywords:

Biowaste-derived biochar  
Phenol degradation  
Syntrophic metabolism  
Direct interspecies electron transfer  
Methanogenesis

### ABSTRACT

In this study, six different types of biochar (based on two feedstocks and three pyrolytic temperatures) were prepared as individual additives for both syntrophic phenol degradation and methanogenesis promotion. The results showed that for phenol degradation, the addition of biochar (15 g/L) shortened the methanogenic lag time from 15.0 days to 1.1–3.2 days and accelerated the maximum CH<sub>4</sub> production rate from 4.0 mL/d to 10.4–13.9 mL/d. Microbial community analysis revealed that the electro-active *Geobacter* was enriched (from 3.8–7.7% to 11.1–23.1%), depending on the type of biochar that was added. This indicates a potential shift of syntrophic phenol metabolism from a thermodynamically unfavorable pathway with H<sub>2</sub> as the interspecies electron transfer mediator to direct interspecies electron transfer (DIET). Integrated analysis of methanogenesis dynamics and the electrochemical properties of biochar showed that compared with electrical conductivity, the electron exchange capacity of biochar was more likely to dominate the DIET process, which was due to the presence of redox-active organic functional groups in biochar. The removal of biochar from the anaerobic system generally prolonged the lag time, revealing the importance of adsorption capacity of biochar to mitigate bio-toxicity of phenol to microbial activity.

\* Corresponding authors.

E-mail addresses: [saiycain56@aliyun.com](mailto:saiycain56@aliyun.com) (Q. Li), [chenrong@xauat.edu.cn](mailto:chenrong@xauat.edu.cn) (R. Chen).

<sup>1</sup> The authors contributed equally to this work.

<https://doi.org/10.1016/j.jhazmat.2019.121726>

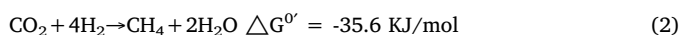
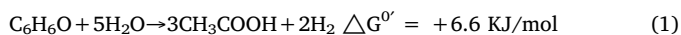
Received 29 May 2019; Received in revised form 18 November 2019; Accepted 19 November 2019

0304-3894/© 2019 Published by Elsevier B.V.

## 1. Introduction

As a hazardous and refractory substance, phenol is commonly found in many types of wastewater generated during industrial processes, such as coking, petroleum-refinement, and dyeing products (Lu et al., 2009; El-Naas et al., 2010; Levén et al., 2012). The efficient removal of phenol and other phenolic pollutants is essential to reduce the bio-toxicity of these industrial effluents into the environment (Jie et al., 2017). Compared with physical, chemical, biological, and their combined treatment processes for phenol (Busca et al., 2008), anaerobic biodegradation has received much attention in recent years, due to its advantages of reduced energy consumption, green biofuel production, and low-cost (Poirier et al., 2018; Rotaru et al., 2014a).

The process of phenol anaerobic degradation involves biological carboxylation, de-aromatized,  $\beta$ -oxidization, and methanogenesis (Fang et al., 2006). Although extensive studies have indicated that different reaction temperatures can influence the degradation pathway, the syntrophic metabolism between phenol oxidizing bacteria and methanogenic archaea is crucial for phenol degradation and methanogenesis (McInerney et al., 2009). Due to the prerequisite of unfavorable thermodynamics of the phenol oxidation (Eq. (1)), this reaction could only have occurred via syntrophic metabolism. As shown in Eq. (2), oxidation of phenol to acetate has to associate with  $H_2$ -scavenging methanogens, which transfer the electron released from the oxidation of phenol to  $CO_2$  for  $CH_4$  production (Gieg et al., 2014; Li et al., 2013). Unfortunately, this syntrophic metabolism with  $H_2$  as the intermediate mediator for interspecies electron transfer (MIET) between bacteria and archaea has been widely studied and proved to be a low-efficient metabolic pathway, which largely limits phenol degradation efficiency in practical applications.



Recently, an alternative pathway for syntrophic metabolism, known as direct interspecies electron transfer (DIET), was confirmed. In the absence of  $H_2$ , specific electro-active microorganisms, such as *Geobacter* and *Shewanella*, can conduct DIET via particular microbial structures and/or substances, such as *e*-pili and cytochrome-*c*, as electron transfer conduits to achieve highly efficient syntrophic metabolism (Lovley, 2017). Moreover, several electrically conductive materials, such as magnetite, granular activated carbon (GAC), carbon nanotubes, graphene, and biochar, were found to be ideal additives for DIET stimulation in syntrophic metabolism (Liu et al., 2012; Wang et al., 2018a; Gilberto et al., 2018; Zhuang et al., 2015; Yan et al., 2018; Zhu et al., 2018). For example, hematite and magnetite promoted methanogenic benzoate degradation by 25 % and 53 % via potential DIET enhancement between syntrophic microbial partners, respectively (Zhuang et al., 2015). What's more, the addition of conductive carbon nanotubes and magnetite nano-particles into an anaerobic system was beneficial for anaerobic phenol degradation and microbial community improvement (Yan et al., 2018). In an upflow anaerobic sludge blanket (UASB) system for coal gasification wastewater treatment, the addition of graphene (0.5 g/L) promoted enhanced the COD removal efficiency and  $CH_4$  production rate, and enrichment with electro-active microbes suggested that DIET was enhanced after graphene addition (Zhu et al., 2018).

Among these materials, biochar produced with bio-waste generally shows a much lower electrical conductivity (EC) property than carbon-based (nano) materials and magnetite. Nevertheless, several studies have reported the potential of biochar to promote syntrophic methanogenesis in anaerobic digestion/degradation systems (Chen et al., 2014; Wang et al., 2018b). The current opinion mostly attributed this influence as below. One the one hand, the potential enrichment of unique functional groups, such as quinones and phenazine, strengthens the redox-active property of biochar, which is beneficial for DIET

between electro-active microbes. Meanwhile, it is also more important than the EC of a material to promote pollutant removal in an electro-chemical system (Prado et al., 2019). Nevertheless, the main mechanism of biochar for promoting syntrophic methanogenesis from phenol is still debatable. In addition, the developed porous 3D structure and high specific surface area (SSA) of biochar are beneficial for both microorganism attachment and pollutant adsorption, which likely accelerate the pollutant biodegradation process. Recent findings indicated that with the help of biochar, *Geobacter* enrichment in an UASB system promoted phenol degradation via DIET (Zhuang et al., 2018; Zhao et al., 2016). However, no evidence is available showing *Geobacter* could be enriched in a suspended sludge system for phenol degradation, even in the presence of conductive substances (Zhuang et al., 2015; Yan et al., 2018).

To fill the afore-mentioned knowledge gaps, in this study, six kinds of biochar were prepared from two feedstock (cattle manure (CM) and sawdust (SD)) and at three pyrolytic temperatures (300 °C, 500 °C, and 700 °C). The effects of each type of biochar on phenol degradation and methanogenesis were investigated separately. By integrating analysis of the methanogenic process, electrochemical properties of biochar and characteristics of the microbial community, the potential mechanism of biochar addition for methanogenic promotion of phenol was elucidated.

## 2. Materials and methods

### 2.1. Biochar preparation and characterization

CM and SD were used as feedstocks for biochar preparation. CM was obtained from a suburban farm, and SD was collected from a local lumber mill. For each feedstock, three type of biochar with particle sizes between 0.25–1 mm were prepared in a muffle under oxygen-limited condition at pyrolytic temperature of 300 °C, 500 °C, and 700 °C, respectively. A detailed protocol of biochar production was shown in our previous study (Wang et al., 2018b). In total, six types of biochar, named CM3, CM5, CM7, SD3, SD5, and SD7, were studied as additive in the anaerobic phenol degradation process, in which "CM" and "SD" were shorten for "Cattle manure" and "Sawdust", and "3, 5, 7" represented the pyrolytic temperatures "300 °C, 500 °C, 700 °C".

The pH value of the biochar was measured in a 5 % (w v<sup>-1</sup>) suspension in deionized water prepared by shaking at 100 rpm under ambient temperature for 24 h using a pH meter (PHS-3C, Dapu Instrument Co., Shanghai, China). Brunauer-Emmett-Teller (BET) SSA was measured via  $N_2$  adsorption multilayer theory by a V-Sorb X800 surface area analyzer (Gold APP Instrument Co., Beijing, China). The elemental (CN/OH) analysis was performed using an isotope ratio mass spectrometer (IRMS, IsoPrime100, Elementar, Germany). Organic functional groups of the biochars were measured with Fourier transform infrared spectroscopy (FT-IR, spectrum two, PerkinElmer, USA) under an attenuated total reflectance (ATR) model. X-ray Photoelectron Spectroscopy (XPS) (K-Alpha, ThermoFisher, USA) was conducted to confirm the organic chemical bond distribution of biochars. The EC of biochar powder was tested with the four-probe method by a powder electrical resistivity tester (ST2722, Jingge, Suzhou, China). Electron accepting capacity (EAC) and electron donating capacity (EDC) of biochar were quantified according to the mediated electrochemical reduction (MER)/oxidation (MEO) method. Electron exchange capacity (EEC) is the sum of EAC and EDC (Zhang et al., 2018). The specific method is described in detail in the Supplementary Information (SI).

### 2.2. Biochar-assisted phenol degradation experiments

According to previous studies, adding degradable substrates into anaerobic phenol degradation system was helpful to achieve rapid phenol degradation startup and accelerate the degradation rate of phenol (Veeresh et al., 2005). Therefore, in this study, a real bio-waste combined with 80 % food wastes and 20 % sewage sludge was used as

co-substrates to explore whether the degradable bio-waste addition could promote phenol degradation. The inoculum used in the experiments was collected from a mesophilic UASB unit of brewery wastewater plant in Xi'an, China. The basic properties of the bio-waste and fresh inoculum were shown in SI.

Batch experiments were conducted with three experimental periods. For the 1<sup>st</sup> period, 20 mL inoculum, 2 mL bio-waste, and 5 mL phenol solution were added to a 120 mL serum bottle. The nutrients solution (SI) was replenished to the total working volume of 90 mL with a phenol concentration of 1 g/L (2.38 g COD/L). After that, each kind of biochar was added to the bottle separately at a dosage of 15 g/L. To investigate whether the degradable bio-waste could promote phenol degradation, two control groups named as "CT1" and "CT2" were operated simultaneously. For CT1, the same volume of bio-waste/phenol solution was added, while for CT2, only the phenol solution was added as substrate. Moreover, a "blank" group without bio-waste and phenol addition was setup to eliminate the impact of biogas produced by the inoculum. After a 40-day duration, 1 g/L phenol was added to all biochar-added and CT2 groups for the 2<sup>nd</sup> period to explore the phenol degradation efficiency of the inoculum after a period of acclimation. The operation of this period was the same as that of 1<sup>st</sup> period. All the experiments were conducted duplicate.

Since the phenol degraded completely in the biochar-added groups during the 2<sup>nd</sup> period, the 3<sup>rd</sup> period was conducted to further investigate the role of biochar in anaerobic system for phenol degradation. Specifically, for each biochar-added group, the mixed sludge filtered with a sterile 60 mesh sieve (pore size with 0.25 mm) to collect the granular biochar. After that, the filtered sludge was divided into two equal parts and was added into two serum bottles. The collected biochar was added into one serum bottle at a dosage of approximately 30 g/L, which has same name with that of 2<sup>nd</sup> period (e.g., CM3). Moreover, the other bottle without biochar addition was setup as a control, and was named "biochar type-CT" (e.g., CM3-CT). All the experiments were conducted in a mesophilic (35 °C) water bath shaker at 120 rpm.

### 2.3. Adsorption of biochar for phenol

To clarify the effect of the adsorption capacity of biochar for phenol in the anaerobic system, all six type of biochar and phenol solution were added to the serum bottle identical to the 1<sup>st</sup> period of phenol degradation, except that the volume of inoculum and bio-waste were substituted with the same volume deionized water. To simulate the condition of anaerobic system, the adsorption experiments were conducted in duplicate under anaerobic condition and operated under 35 °C.

### 2.4. Analytical methods

The average experimental data of each group (2<sup>nd</sup> period and 3<sup>rd</sup> period) for methanogenesis was fitted by the modified Gompertz equation:

$$P = P_0 \cdot \exp \left\{ -\exp \left[ \frac{R_{\max} \cdot e}{P_0} \cdot (t_0 - t) + 1 \right] \right\}$$

where P represents CH<sub>4</sub> production (mL), P<sub>0</sub> represents CH<sub>4</sub> production potential (mL), R<sub>max</sub> represents the maximum CH<sub>4</sub> production rate (mL/d), t<sub>0</sub> represents the lag time (days), and e = 2.718281828. Origin 8.0 software (OriginLab Corporation, USA) was used to simulate the CH<sub>4</sub> production curve and to fit the results. The significance of microbial community differentiation was analyzed with One-way Analysis of Variation (ANOVA) by SPSS 10.0 (International Business Machines Corporation, NY, USA).

The biogas production volume was measured with a glass syringe. The biogas composition, including H<sub>2</sub>, CH<sub>4</sub> and CO<sub>2</sub>, was monitored by a gas chromatograph (GC) (GC7900, Tianmei, China) equipped with a thermal conductivity detector (TCD) and a molecular sieve packed stainless steel column (TDX-01, Shanghai Xingyi Chrome, China). Argon gas was used as carrier gas for measurement. The CH<sub>4</sub> production was calculated by adding the CH<sub>4</sub> volume in glassy syringe and in the headspace. Phenol and VFAs was monitored by a GC (PANNO, China) equipped with a flame ionization detector (FID) and DB-FFAP column (φ 0.32 mm × 50 m; Agilent, USA).

### 2.5. Microbial community analysis

To elucidate the mechanisms of biochar addition for phenol degradation promotion, microbial community of both archaea and bacteria were analyzed at the end of 1<sup>st</sup> reaction period. The high-throughput sequencing method was used for microbial community analysis (Wang et al., 2018b).

For DNA extraction, the sludge samples were centrifuged at 13,000 rpm for 10 min, and then the pellets were rinsed with phosphate buffering saline twice. After that, the PowerSoil® DNA Isolation Kit (MO BIO, USA) was used for DNA extraction, according to the manufacturer's instruction. The extracted DNA samples were stored in -20 °C environment for conservation for further analysis.

An Illumina platform (Illumina Miseq PE250, Sangon Biotech, Shanghai, China) was employed for high-throughput sequencing analysis of both bacterial and archaeal community. For the bacteria, the universal primers 515 F (5'-GTGCCAGCMGCCGCGTAA-3') and 806R (5'-GGACTACHVGGGTWCTAAT-3') were used for amplifying V4 regions of 16S rRNA gene via PCR. For the archaea, the two-cycle nested PCR was used to amplifying V3-V4 regions of 16S rRNA gene. In the first cycle, the primers 340 F (5'-CCCTAYGGGGYGCASCAG-3') and 1000R (5'-GGCCATGCACYWCYTCTC-3') were used. The primers 349 F (5'-GYGCASCAGKCGMGAAW-3') and 806R (5'-GGACTACHVGGGTWCTAAT-3') were used for the second cycle. As the amplification process ended, the PCR products were examined via agarose gel electrophoresis to determine the quality of amplification. After purification with Agencourt AMPure XP magnetic beads (Backman Coulter, USA), the PCR products were quantified by a Qubit 2.0 DNA detection kit (Sangon Biotech, Shanghai, China).

**Table 1**  
Physico-chemical properties of biochars.

Parameter	CM3	CM5	CM7	SD3	SD5	SD7
Ash content (wt%)	15.4 ± 0.2	19.9 ± 0.6	22.6 ± 0.5	5.3 ± 0.3	7.8 ± 0.7	15.0 ± 0.2
pH in solution	7.6 ± 0.1	8.5 ± 0.1	8.9 ± 0.1	7.3 ± 0.1	9.2 ± 0.1	10.0 ± 0.2
specific surface area (m <sup>2</sup> /g)	4.2 ± 0.3	9.4 ± 2.5	77.8 ± 6.7	9.2 ± 2.1	83.6 ± 3.9	181.3 ± 5.4
C (wt%)	42.3 ± 1.9	43.9 ± 0.4	49.4 ± 2.6	66.6 ± 1.8	74.5 ± 0.6	78.8 ± 1.1
N (wt%)	1.9 ± 0.	1.7 ± 0.1	1.2 ± 0.2	0.4 ± 0.0	0.4 ± 0.0	0.4 ± 0.1
H (wt%)	3.6 ± 0.1	2.0 ± 0.1	1.2 ± 0.1	6.9 ± 0.5	4.8 ± 0.3	3.9 ± 0.2
O (wt%)	23.4 ± 0.6	19.2 ± 0.3	15.9 ± 0.6	18.5 ± 0.8	12.2 ± 0.6	10.9 ± 0.1

### 3. Results and discussion

#### 3.1. Effects of feedstock and pyrolytic temperature on physical and electrochemical characteristics of biochar

According to Table 1 and SI, the physico-chemical characteristics of biochar varied depending on both the pyrolytic temperature and feedstock used for production. SD biochar contained more diversified organic functional groups (such as  $(\text{CH}_2)_n$ , aliphatic C–O, C=C, and aromatic structures) compared with CM biochar (Trigo et al., 2016; Kan et al., 2016) (SI). The organic chemical bond of C1s and O1s detected in the survey scan spectrum indicated that carbon and oxygen were the main elements for both CM biochar and SD biochar (SI), and the ratio of O/C decreased as the pyrolytic temperature increased due to the enhancement of the carbonization degree (Keiluweit et al., 2010). For the specific C1s spectra of all biochar, the peak at the binding energy of 284.5 eV was C–C/C=C, which could be attributed to the graphitic structure of carbonization (Zhang et al., 2018). The higher relative area of this peak, as the pyrolytic temperature increased, implies the transformation of organic structure from the aliphatic/aromatic form to the condensed sheet graphitic form. The comparison between O containing groups of CM biochar and SD biochar showed that the relatively higher O content of CM biochar was likely attributed to the O–C=O (carboxyl) group. However, SD biochar contained higher content of carbonyl groups, especially for the biochar produced under 300 °C and 500 °C. The C=O structure bound to the benzene ring could form important electron shuttle structures, such as quinone and hydroquinone, to assist interspecies electron transfer via the redox reaction (Yuan et al., 2017).

As two potential characteristics associating with DIET, the redox-based EEC and EC of each type of biochar were compared in Figs. 1 and 2. Mediated electrochemical analysis showed that the EAC mostly dominated the EEC of biochar (Fig. 1). The highest EEC of SD biochar

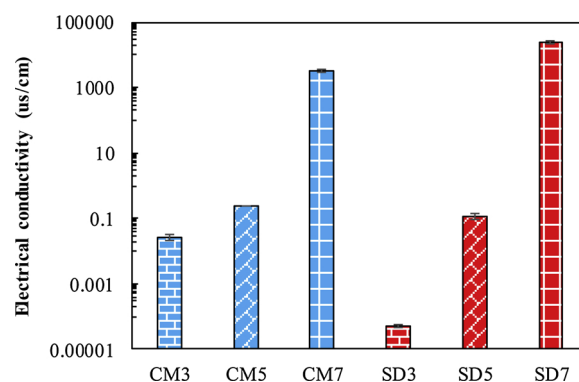


Fig. 2. Electrical conductivity of different kinds of biochar.

was  $6.57 \mu\text{mol e}^-/\text{g}$  biochar produced at 500 °C, which could have been attributed to the enriched quinone functional groups at this pyrolytic temperature (Klöpffel et al., 2014). However, both the EAC and EEC of CM biochar showed decreasing trends as the pyrolytic temperature increased, which was likely due to a variation in the O content (Zhang et al., 2018). For the biochar produced with the same feedstock, EC increased as pyrolytic temperature increased, which was consistent with the continued growth and condensation of graphitic crystallites (Gabhi et al., 2017) (Fig. 2). A comparison between SD biochar and CM biochar confirmed that SD biochar showed a more significant variation range with changing pyrolytic temperature, suggesting a strong influence of the organic carbon-based structure on the EC of biochar.

#### 3.2. Effects of biochar addition on anaerobic phenol degradation

During the 1<sup>st</sup> period, degradable bio-waste was used to facilitate phenol degradation. However, unlike the positive results reported in

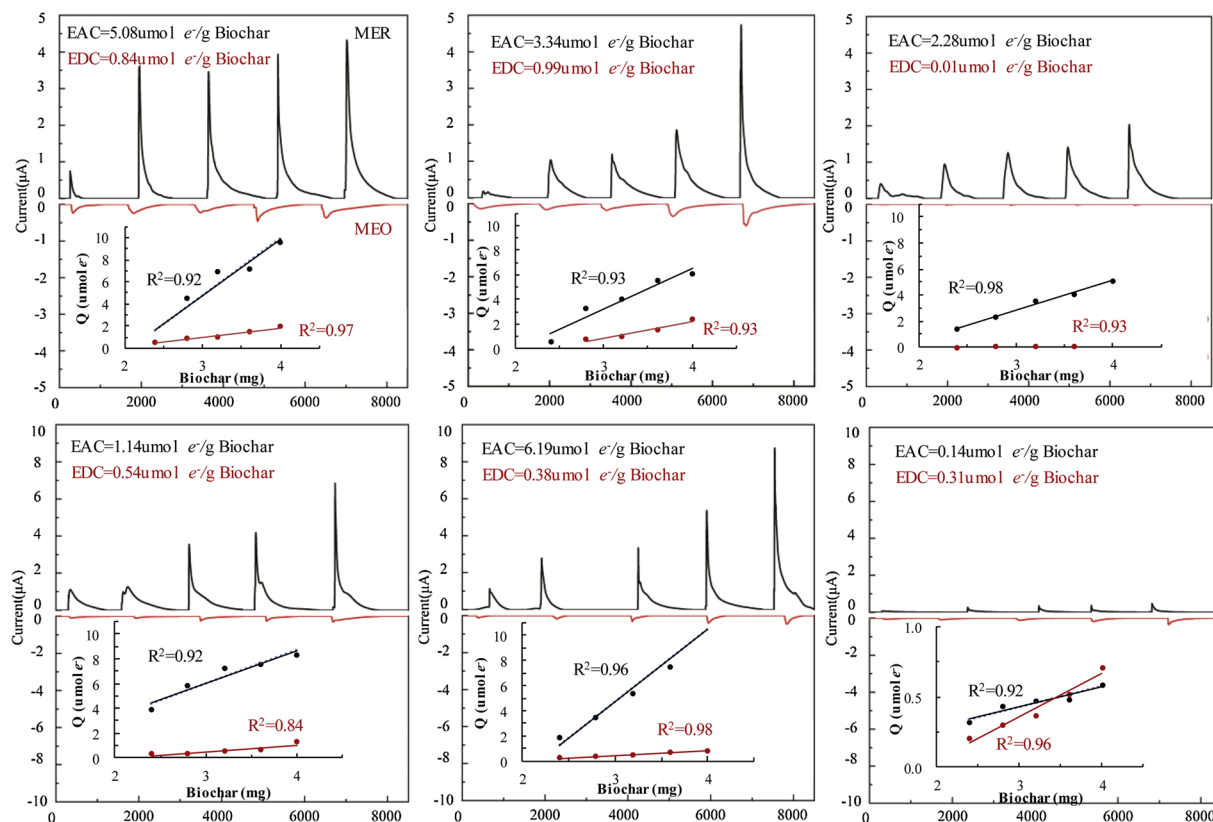


Fig. 1. Electrochemical analysis of electron accepting capacity (EAC) and electron donating capacity (EDC) of CM3 (a), CM5 (b), CM7 (c), SD3 (d), SD5 (e) and SD7 (f).

previous studies (Poirier et al., 2018; Rotaru et al., 2014a), the current results found that CT1 with the addition of degradable bio-waste had a much longer lag phase for phenol degradation compared with CT2 (substrate was only phenol). This indicates few benefits for the addition of degradable bio-waste to accelerate phenol degradation (Fig. 3(a, b)). The reason was likely associated with the microbial community succession, which is discussed in details in Section 3.3.

Compared with the two control groups, all biochar-added groups showed methanogenic promotion of phenol. Due to the adsorption of biochar (Fig. 3(b)), phenol concentration rapidly decreased on the 1<sup>st</sup> day of the reaction to different degrees (Rotaru et al., 2014a). Adsorption experiments confirmed that the adsorption capacity of biochar ranged between 24.4 mg phenol/g biochar and 62.8 mg phenol/g biochar, depending on the type of biochar (SI). For identical pyrolytic temperatures, the higher adsorption capacity of SD biochar was likely attributed to the higher SSA (Table 1).

Results of the 2<sup>nd</sup> period with phenol as the sole substrate indicated

that after a period of acclimation, the methanogenesis of phenol in the biochar-added groups was completed in 16 days (Fig. 3 (c, d)). For CT2, however, the lag time was longer than that of 1<sup>st</sup> period, suggesting that in the absence of biochar, the lasting bio-toxicity of phenol strongly inhibited the methanogenesis process, even after one period of microbial acclimation. Compared with CT2 in the 1<sup>st</sup> period, the lag time of biochar added groups was shortened from 15.0 days to 1.1–3.0 days, whereas the  $R_{max}$  increased from 4.0 mL/day to 10.4–13.9 mL/day, indicating that microbial activity was greatly enhanced in the presence of biochar (SI).

The 3<sup>rd</sup> period experiment was conducted to clarify the effect of removing biochar on phenol degradation dynamics after two periods microbial acclimation. The results indicated that the lag time of methanogenesis was prolonged in the absence of biochar. However, the  $R_{max}$  of each control group was still comparable with that of the respective biochar-added group during the 2<sup>nd</sup> period (changed from -32.4%–15.4%) (Fig. 3(e, f) and Fig. 4). Although the removal of

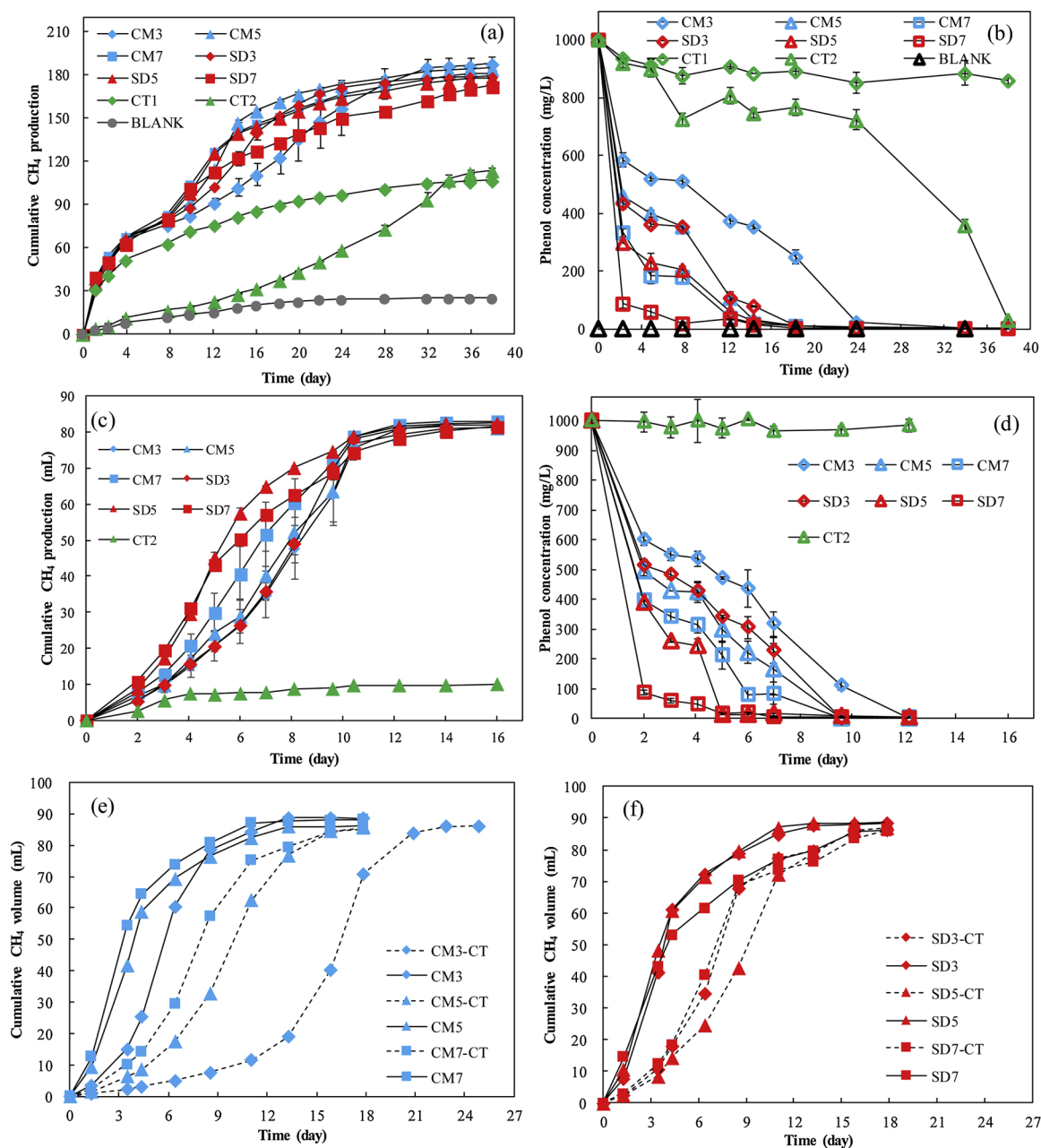


Fig. 3. CH<sub>4</sub> production and phenol concentration variation in 1<sup>st</sup> period (a, b), 2<sup>nd</sup> period (c, d) and 3<sup>rd</sup> period (e, f).

biochar from the anaerobic system forced microbes to degrade soluble phenol for metabolism, the degradation rate was virtually unaffected. Clearly, after two periods of acclimation, the microbes for phenol degradation that existed in the suspended sludge facilitated the degradation of phenol, even in the absence of biochar. After comparing the groups in which biochar was removed, most biochar-added groups in the 3<sup>rd</sup> period showed further significant benefits for lag time shortening and  $R_{max}$  acceleration, suggesting an important role of biochar for methanogenic promotion, even in cases of well-acclimated microbial communities (Fig. 4).

### 3.3. Effects of biochar addition on microbial community characteristics

Microbial samples were collected at the end of the 1<sup>st</sup> period. The results in Fig. 5 (a) illustrated that for the inoculum, two fermentative bacteria, *Thermogutta* and *Levilinea*, were the dominant genera in the bacterial community. However, their relative abundances decreased from 46.1 % and 8.6 % to 0.2–0.6 % and less than 0.1 %, respectively, in the biochar-added and two control groups (Fig. 5), indicating that the acclimation of substrates significantly altered the microbial community. Furthermore, the relative abundance of *Geobacter* was largely enriched after phenol acclimation. Noticeably, although *Geobacter* were reported as important functional bacteria in granular sludge for DIET achievement in brewery wastewater treatment units, it had extremely low relative abundance in the inoculum. This was possibly due to the poor granulation conditions of sludge in the inoculum used in this study (Rotaru et al., 2014b). Our previous studies with the same bio-waste and inoculum for anaerobic digestion under the mesophilic condition showed that both batch and long-term semi-continuous operation models could not enrich the electro-active *Geobacter*. This suggests that the bio-wastes used in this study were not the inducing factor for *Geobacter* enrichment ((Wang et al., 2018b) and data not been published). Moreover, the degradation of phenol and the higher relative abundance of *Geobacter* in CT2 compared with that of CT1 also indicated that the enrichment of high-efficient functional bacteria was more significant than the addition of degradable bio-waste to promote phenol degradation. The results of ANOVA for comparing the differences between the biochar-added and two control groups indicated that biochar addition significantly enhanced the enrichment of *Geobacter* ( $p < 0.05$ ). *Syntrophorhabdus* is another functional metabolizer that can degrade phenol to acetate in syntrophic associations with hydrogenotrophic methanogens through the thermodynamically unfavorable electron transfer process (Qiu et al., 2008). The genus of *Syntrophorhabdus* was not detected in the inoculum, and just accounted for 1.1 % and 2.1 % in CT1 and CT2, respectively. However, as biochar was added, its relative abundance increased to 3.4%–9.3%, respectively, which was consistent with the promotion of phenol degradation in the biochar-added groups.

The analysis of archaeal communities, as illustrated in Fig. 5(b), indicated that the archaeal communities varied slightly after phenol acclimation compared with bacterial communities. *Methanosaeta* and *Methanobacterium* were two main genera, accounting for 88.9–99.5 % of the total archaeal community. However, the relative abundance of *Methanosaeta* increased from 49.2 % and 49.8 % in CT2 and CT1 to 66.5–76.1 % in biochar-added groups, respectively, indicating that *Methanosaeta*, but not *Methanobacterium*, played the determining role for the highly efficient methanogenesis of phenol. As an archaeal genus that can directly accept electrons from electron mediator or electro-active bacteria, the enrichment of *Methanosaeta* during DIET has been widely reported (Zhao et al., 2017; Wang et al., 2016). In a brewery wastewater digester, DIET between *Geobacter* and *Methanosaeta* was observed, and the authors claimed that the released electrons of *Geobacter* were transferred to *Methanosaeta* via electrically conductive pili for CO<sub>2</sub> reduction (Rotaru et al., 2014b). Another study with phenol as the sole substrate for anaerobic degradation (Yan et al., 2018) reported that adding nano-materials (carbon nanotubes and magnetite) enriched

*Methanosaeta* from 30.99 % to 40.36–46.33 % and decreased the relative abundance of *Methanobacterium* from 56.26 % to 31.27–36.66 %, which was consistent with the results of the present study. Furthermore, a UASB reactor for coal gasification wastewater treatment confirmed that the addition of electrically conductive graphene enhanced COD removal and CH<sub>4</sub> production via DIET between *Geobacter* and *Methanosaeta* (Zhu et al., 2018). Therefore, according to the variations in the microbial communities in this study, it is reasonable to postulate that different metabolic types of phenol degradation occurred. On the other hand, for CT2, syntrophic metabolism between *Syntrophorhabdus* and *Methanobacterium* with H<sub>2</sub> as the electron transfer mediator likely triggered the degradation of phenol (Franchi et al., 2018). However, this thermodynamically unfavorable electron transfer process greatly limited the metabolic efficiency (Nobu et al., 2014). In biochar-added groups, the addition of biochar strengthened the low-efficient metabolic pathway in control groups through *Syntrophorhabdus* enrichment. More importantly, it also triggered the thermodynamically favorable syntrophic metabolism between *Geobacter* and *Methanosaeta*, potentially via DIET, to achieve the high-efficient methanogenesis of phenol.

### 3.4. Potential mechanisms of biochar addition for phenol degradation promotion

According to the results of the three periods and microbial community analysis, it is believed that biochar addition promoted the methanogenesis of phenol via both the strong adsorption capacity for phenol and syntrophic DIET enhancement of microbial communities. As a carbon-based porous material, biochar has been confirmed to be an adsorbent for the hydrophobic phenolic substance removal from aqueous environments (Girods et al., 2009; Li et al., 2017). Although building an adsorption-biodegradation model in an anaerobic system via addition of adsorptive materials is beneficial for the promotion of phenol degradation, the associated mechanisms still remain unclear (Rotaru et al., 2014a). Thus, to confirm whether EC or EEC of biochar exerted a greater influence on the enhancement of DIET, the relationship between the methanogenesis process and the physical or electro-chemical properties of biochar were analyzed by linear correlations. The results (Fig. 6) indicated that the lag time of methanogenesis had a strong linear relationship with the adsorption capacity of biochar ( $R^2 = 0.91$ ). As a bio-toxic substance, the soluble phenol in the anaerobic system could inhibited the metabolic activity (Fang and Chan, 1997). The importance of the adsorption capacity of biochar for triggering phenol degradation could be attributed to two possible reasons. Firstly, the conversion of phenol from soluble form to adsorptive form via the addition of biochar mitigated the bio-toxicity of phenol to microbes. More importantly, adsorptive phenol was more accessible for the attached microbes in biochar to degrade via a favorable

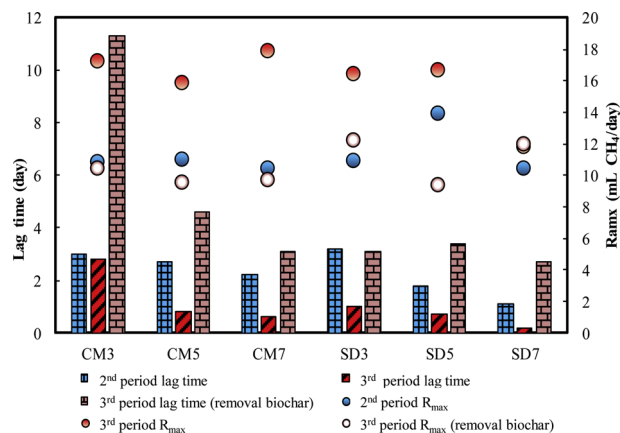


Fig. 4. Comparisons of lag time and  $R_{max}$  of methane production fitted by modified Gompertz equation in 2nd and 3rd periods.

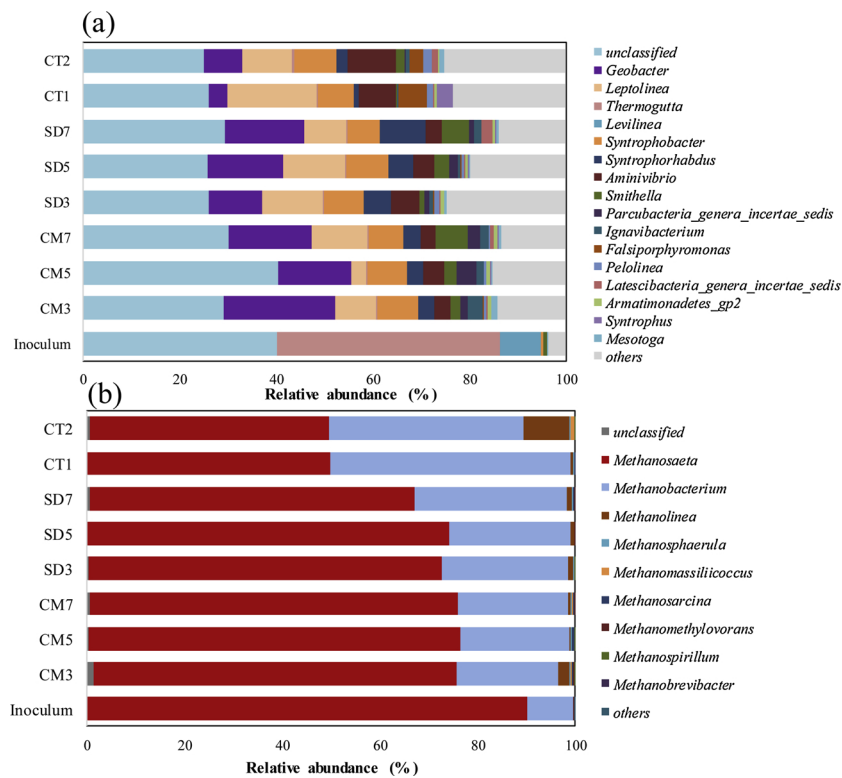


Fig. 5. Relative abundance of bacteria (a) and archaea (b) at genus level.

thermodynamic process (DIET) (Shrestha et al., 2013). Secondly, after comparing the EC and EEC of biochar, the EEC showed a more positive linear relationship with the  $R_{\max}$  of methanogenesis ( $R^2 = 0.4634$  vs  $R^2 = 0.0985$ ). This finding suggested that even the methanogenesis process was not completely controlled by the EEC of added biochar due to the slightly linear relationship, the role of biochar as the redox-active mediator was more dominant than as an electrical conductor to stimulate DIET between electro-active bacteria and methanogens for syntrophic phenol oxidation. Although the biochar used in this study showed poor EC (Zhang et al., 2018), the enriched redox-active functional groups existing in biochar were beneficial for the promotion of biological electron transfer between electro-active microbes via its

redox-active organic functional groups (SI) (Saquing et al., 2016; Beckmann et al., 2016). In our previous study, the capacity of biochar to act as electron acceptors for syntrophic oxidation was confirmed, even in the absence of methanogenesis (Wang et al., 2018b). In this study, FT-IR and XPS analysis indicated that quinone and hydro-quinone-related functional groups potentially existed on the surface of biochar, and SD-derived biochar produced at 500 °C seemed to contain the highest contents, which was consistent with the highest  $R_{\max}$  performance of methanogenesis.

Compared with the methanogenesis process and microbial community of 2<sup>nd</sup> and 3<sup>rd</sup> periods (Fig. 4), it was found that the removal of biochar did not significantly influence  $R_{\max}$ . However, it prolonged the

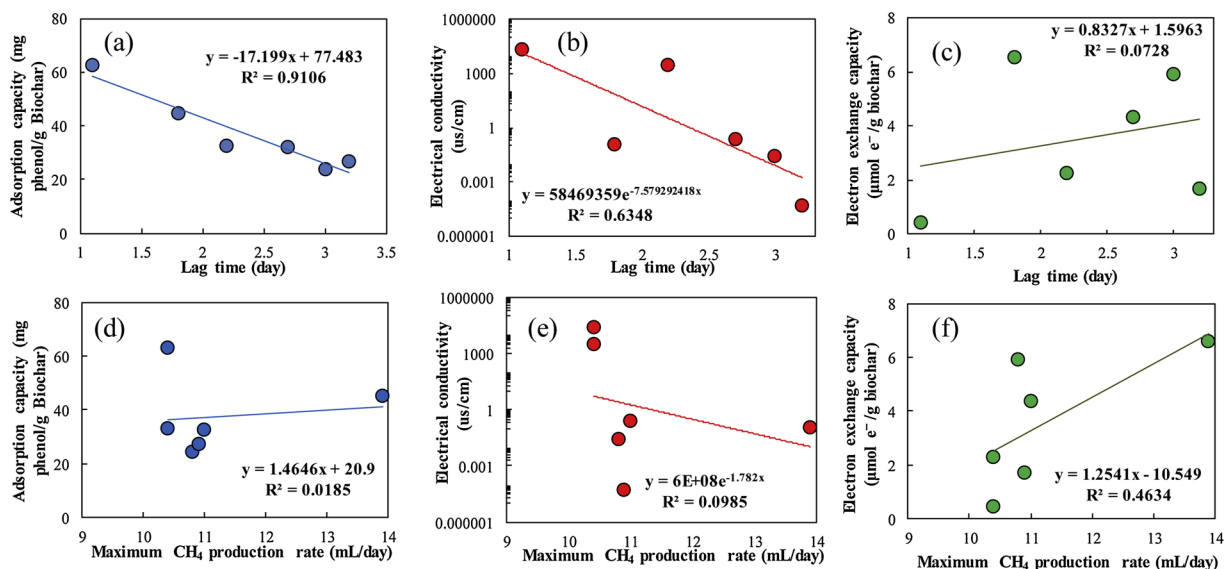


Fig. 6. Correlation between methanogenic lag time (a, b, c), and maximum  $\text{CH}_4$  production rate (d, e, f) and adsorption capacity or electrochemical properties of biochar.

lag time, suggesting the negative impact of soluble phenol on microbes. Although the well-acclimated microbial community was reshaped with the assistance of biochar after two reaction periods, a transformation of bio-toxic phenol from adsorptive form to soluble form caused an acute environmental shock for the microorganisms. According to the results of microbial community analysis, it is believed that even in the absence of biochar, acclaimed electro-active syntrophic partners (*Geobacter* and *Methanosaeta*) could also achieve potential DIET via e-pili connection or cytochrome-c mediation (Fig. 5) (Rotaru et al., 2014b). Fortunately, the further significant benefits for the lag time shortening and  $R_{max}$  acceleration of biochar-added groups during the 3<sup>rd</sup> period confirmed that besides the adsorption for bio-toxic reduction, the more important role of biochar was as a redox-active mediator to stimulate a more highly efficient DIET, rather than that occurring between syntrophic partners themselves. In summary, the potential mechanisms of biochar-assisted phenol degradation for methanogenesis can be described as follows. Firstly, the introduction of biochar transfers a proportion of the phenol from the soluble form to the adsorptive form, which is beneficial for bio-toxicity reduction. Furthermore, the redox-active property of biochar enriched the growth of electro-active bacteria (*Geobacter*) and archaea (*Methanosaeta*). Biochar accepted the electrons released from phenol oxidation by bacteria first, and then transferred them to methanogenic archaea for methanogenesis through CO<sub>2</sub> reduction. In this way, highly efficient syntrophic phenol oxidation based on DIET is established for methanogenesis.

As a sustainable material, biochar can be produced from diverse bio-waste. Moreover, during pyrolysis, the extracted bio-oil and syngas produced simultaneously with biochar preparation could be *in-situ* combusted for combined heat and power (CHP) production. This means that in addition to biochar production, extra renewable energy could be produced during pyrolysis without positive GHG emission (Peters et al., 2015). In a recent report, the impact of biochar production and use at the city-scale for climate change mitigation was evaluated via life cycle assessment, and the results showed that compared with the current scenarios with forest biomass as energy source, an integrated CHP system with pyrolysis and biochar comprehensive utilization was more beneficial for climate change mitigation, especially in a long-term duration-based evaluation (Azzi et al., 2019). Consequently, we believe that the biochar-assisted phenol degradation proposed in this study has a promising future for the sustainable treatment of phenol wastewater.

#### 4. Conclusions

The results of this study showed that the addition of biochar accelerated the syntrophic oxidation of phenol for methanogenesis in an anaerobic system. Typical electro-active microbes (*Geobacter* and *Methanosaeta*) were enriched with the assistance of biochar, indicating that highly efficient syntrophic phenol degradation was stimulated by the potential DIET pathway. The electron exchange capacity of biochar seemed to be more significant than that of the electrical conductivity for DIET enhancement. Meanwhile, the adsorption capacity of biochar for phenol was significant for mitigating bio-toxicity of phenol to microbial activity. In summary, this study proposed a green and low-cost strategy for the rapid methanogenesis of phenol, which could be meaningful for the sustainable treatment of hazardous phenol-containing wastewater.

#### Declaration of Competing Interest

The authors declare that they have no known competing financial interests or personal relationships that could have appeared to influence the work reported in this paper.

#### Acknowledgements

This work was supported by National Natural Science Foundation of

China (Grant No. 51978560, 51608430), National Key Research and Development Project (No. 2017YFE0127300), and Shaanxi Provincial Program for Innovative Research Team (No. 2019TD-025).

#### Appendix A. Supplementary data

Supplementary material related to this article can be found, in the online version, at doi:<https://doi.org/10.1016/j.jhazmat.2019.121726>.

#### References

- Azzi, E.S., Karlton, E., Sundberg, C., 2019. Prospective life cycle assessment of large-scale biochar production and use for negative emissions in Stockholm. *Environ. Sci. Technol.* 53, 8466–8476.
- Beckmann, S., Welte, C., Li, X., Oo, Y.M., Kroeninger, L., Heo, Y., Zhang, M., Ribeiro, D., Lee, M., Bhadbhade, M., 2016. Novel phenazine crystals enable direct electron transfer to methanogens in anaerobic digestion by redox potential modulation. *Synth. Lect. Energy Environ. Technol. Sci. Soc.* 9, 644–655.
- Busca, G., Berardinelli, S., Resini, C., Arrighi, L., 2008. Technologies for the removal of phenol from fluid streams: a short review of recent developments. *J. Hazard. Mater.* 160, 265–288.
- Chen, S., Rotaru, A.E., Shrestha, P.M., Malvankar, N.S., Liu, F., Fan, W., Nevin, K.P., Lovley, D.R., 2014. Promoting interspecies electron transfer with biochar. *Sci. Rep.* 4, 5019.
- El-Naas, M.H., Al-Zuhair, S., Alhajja, M.A., 2010. Removal of phenol from petroleum refinery wastewater through adsorption on date-pit activated carbon. *Chem. Eng. J.* 162, 997–1005.
- Fang, H.H.P., Chan, O.C., 1997. Toxicity of phenol towards anaerobic biogranules. *Water Res.* 31, 2229–2242.
- Fang, H.H.P., Liang, D.W., Zhang, T., Liu, Y., 2006. Anaerobic treatment of phenol in wastewater under thermophilic condition. *Water Res.* 40, 427–434.
- Franchi, O., Bovio, P., Ortega-Martínez, E., Rosenkranz, F., Chamy, R., 2018. Active and total microbial community dynamics and the role of functional genes *bamA* and *mcrA* during anaerobic digestion of phenol and *p*-cresol. *Bioresour. Technol.* 264, 290–297.
- Gabhi, R.S., Kirk, D.W., Jia, C.Q., 2017. Preliminary investigation of electrical conductivity of monolithic biochar. *Carbon* 116, 435–442.
- Gieg, L.M., Fowler, S.J., Berdugo-Lavijio, C., 2014. Syntrophic biodegradation of hydrocarbon contaminants. *Curr. Opin. Biotechnol.* 27, 21–29.
- Gilberto, M., Filipa, S.A., Luciana, P., Madalena, A.M., 2018. Methane production and conductive materials: a critical review. *Environ. Sci. Technol.* 52, 10241–10253.
- Girods, P., Dufour, A., Fierro, V., Rogaume, Y., Rogaume, C., Zoualalian, A., Celzard, A., 2009. Activated carbons prepared from wood particleboard wastes: Characterisation and phenol adsorption capacities. *J. Hazard. Mater.* 166, 491–501.
- Jie, L., Park, J., Pandey, L.K., Choi, S., Lee, H., Saeger, J.D., Depuydt, S., Han, T., 2017. Testing the toxicity of metals, phenol, effluents, and receiving waters by root elongation in *Lactuca sativa* L. *Ecotox. Environ. Safe.* 149, 225–232.
- Kan, T., Strezov, V., Evans, T.J., 2016. Lignocellulosic biomass pyrolysis: a review of product properties and effects of pyrolysis parameters. *Renew. Sustain. Energ. Rev.* 57, 1126–1140.
- Keiluweit, M., Nico, P.S., Johnson, M.G., Kleber, M., 2010. Dynamic molecular structure of plant biomass-derived black carbon (biochar). *Environ. Sci. Technol.* 44, 1247–1253.
- Klüpfel, L., Keiluweit, M., Kleber, M., Sander, M., 2014. Redox properties of plant biomass-derived black carbon (Biochar). *Environ. Sci. Technol.* 48, 5601–5611.
- Levén, L., Nyberg, K., Schnürer, A., Sastreconde, I., Poggivaldo, H., Lobo, M.C., Sanz, J.L., Macarie, H., 2012. Conversion of phenols during anaerobic digestion of organic solid waste - a review of important microorganisms and impact of temperature. *J. Environ. Manage.* 95, S99–S103.
- Li, Z., Inoue, Y., Suzuki, D., Ye, L., Katayama, A., 2013. Long-term anaerobic mineralization of pentachlorophenol in a continuous-flow system using only lactate as an external nutrient. *Environ. Sci. Technol.* 47, 1534–1541.
- Li, H., Mahyoub, S.A.A., Liao, W., Xia, S., Zhao, H., Guo, M., Ma, P., 2017. Effect of pyrolysis temperature on characteristics and aromatic contaminants adsorption behavior of magnetic biochar derived from pyrolysis oil distillation residue. *Bioresour. Technol.* 223, 20–26.
- Liu, F., Rotaru, A.E., Shrestha, P.M., Malvankar, N.S., Nevin, K.P., Lovley, D.R., 2012. Promoting direct interspecies electron transfer with activated carbon. *Environ. Sci. Technol.* 46, 8982–8989.
- Lovley, D.R., 2017. Syntrophy Goes electric: direct interspecies Electron transfer. *Annu. Rev. Microbiol.* 71, 643–664.
- Lu, Y., Yan, L., Wang, Y., Zhou, S., Fu, J., Zhang, J., 2009. Biodegradation of phenolic compounds from coking wastewater by immobilized white rot fungus *Phanerochaete chrysosporium*. *J. Hazard. Mater.* 165, 1091–1097.
- McInerney, M.J., Sieber, J.R., Gunsalus, R.P., 2009. Syntrophy in anaerobic global carbon cycles. *Curr. Opin. Biotechnol.* 20, 623–632.
- Nobu, M.K., Narihiro, T., Tamaki, H., Qiu, Y.L., Sekiguchi, Y., Woyke, T., Goodwin, L., Davenport, K.W., Kamagata, Y., Liu, W.T., 2014. Draft genome sequence of *Syntrophorhabdus aromaticivorans* strain UI, a mesophilic aromatic compound-degrading syntroph. *Genome Announc.* 2, e01064–13.
- Peters, J.F., Diego, L., Javier, D., 2015. Biomass pyrolysis for biochar or energy applications? A life cycle assessment. *Environ. Sci. Technol.* 49, 5195–5202.
- Poirier, S., Déjean, S., Chapleur, O., 2018. Support media can steer methanogenesis in the

- presence of phenol through biotic and abiotic effects. *Water Res.* 140, 24–33.
- Prado, A., Berenguer, R., Esteve-Núñez, A., 2019. Electroactive biochar outperforms highly conductive carbon materials for biodegrading pollutants by enhancing microbial extracellular electron transfer. *Carbon* 146, 597–609.
- Qiu, Y., Hanada, S., Ohashi, A., Harada, H., Kamagata, Y., Sekiguchi, Y., 2008. *Syntrophorhabdus aromaticivorans* gen. nov., sp. nov., the first cultured anaerobe capable of degrading phenol to acetate in obligate syntrophic associations with a hydrogenotrophic methanogen. *Appl. Environ. Microbiol.* 74, 2051–2058.
- Rotaru, A.E., Shrestha, P.M., Liu, F., Shrestha, M., Shrestha, D., Embree, M., Zengler, K., Wardman, C., Nevin, K.P., Lovley, D.R., 2014a. A new model for electron flow during anaerobic digestion: direct interspecies electron transfer to *Methanosaeta* for the reduction of carbon dioxide to methane. *Energ. Environ. Sci.* 7, 408–415.
- Rotaru, A.E., Shrestha, P.M., Liu, F., Shrestha, M., Shrestha, D., Embree, M., Zengler, K., Wardman, C., Nevin, K.P., Lovley, D.R., 2014b. A new model for electron flow during anaerobic digestion: direct interspecies electron transfer to *Methanosaeta* for the reduction of carbon dioxide to methane. *Energ. Environ. Sci.* 7, 408–415.
- Saquin, J.M., Yu, Y.H., Pei, C.C., 2016. Wood-derived black carbon (Biochar) as a microbial Electron donor and acceptor. *Environ. Sci. Technol. Lett.* 3, 62–66.
- Shrestha, P.M., Rotaru, A.E., Aklujkar, M., Liu, F., Shrestha, M., Summers, Z.M., Malvankar, N., Dan, C.F., Lovley, D.R., 2013. Syntrophic growth with direct interspecies electron transfer as the primary mechanism for energy exchange. *Environ. Microbiol. Rep.* 5, 904–910.
- Trigo, C., Cox, L., Spokas, K., 2016. Influence of pyrolysis temperature and hardwood species on resulting biochar properties and their effect on azimsulfuron sorption as compared to other sorbents. *Sci. Total Environ.* 566–567, 1454–1464.
- Veeresh, G.S., Kumar, P., Mehrotra, I., 2005. Treatment of phenol and cresols in upflow anaerobic sludge blanket (UASB) process: a review. *Water Res.* 39, 154–170.
- Wang, L.Y., Nevin, K.P., Woodard, T.L., Mu, B.Z., Lovley, D.R., 2016. Expanding the diet for DIET: electron donors supporting direct interspecies Electron transfer (DIET) in defined Co-cultures. *Front. Microbiol.* 7, 236.
- Wang, T., Zhang, D., Dai, L., Dong, B., Dai, X., 2018a. Magnetite triggering enhanced DIET: a scavenger for the blockage of Electron transfer in anaerobic digestion of high-solids sewage sludge. *Environ. Sci. Technol.* 52, 7160–7169.
- Wang, G., Li, Q., Gao, X., Wang, X.C., 2018b. Synergetic promotion of syntrophic methane production from anaerobic digestion of complex organic wastes by biochar: performance and associated mechanisms. *Bioresour. Technol.* 250, 812–820.
- Yan, W., Sun, F., Liu, J., Yan, Z., 2018. Enhanced anaerobic phenol degradation by conductive materials via EPS and microbial community alteration. *Chem. Eng. J.* 352, 1–9.
- Yuan, Y., Bolan, N., Prévosteau, A., Vithanage, M., Biswas, J.K., Ok, Y.S., Wang, H., 2017. Applications of biochar in redox-mediated reactions. *Bioresour. Technol.* 246, 271–281.
- Zhang, P., Zheng, S., Liu, J., Wang, B., Liu, F., Feng, Y., 2018. Surface properties of activated sludge-derived biochar determine the facilitating effects on *Geobacter* co-cultures. *Water Res.* 142, 441–451.
- Zhao, Z., Zhang, Y., Holmes, D.E., Yan, D., Woodard, T.L., Nevin, K.P., Lovley, D.R., 2016. Potential enhancement of direct interspecies electron transfer for syntrophic metabolism of propionate and butyrate with biochar in up-flow anaerobic sludge blanket reactors. *Bioresour. Technol.* 209, 148–156.
- Zhao, Z., Li, Y., Yu, Q., Zhang, Y., 2017. Ferroferric oxide triggered possible direct interspecies electron transfer between *Syntrophomonas* and *Methanosaeta* to enhance waste activated sludge anaerobic digestion. *Bioresour. Technol.* 250, 79–86.
- Zhu, H., Han, Y., Ma, W., Han, H., Ma, W., Xu, C., 2018. New insights into enhanced anaerobic degradation of coal gasification wastewater (CGW) with the assistance of graphene. *Bioresour. Technol.* 262, 302–309.
- Zhuang, L., Tang, J., Wang, Y., Hu, M., Zhou, S., 2015. Conductive iron oxide minerals accelerate syntrophic cooperation in methanogenic benzoate degradation. *J. Hazard. Mater.* 293, 37–45.
- Zhuang, H., Zhu, H., Shan, S., Zhang, L., Fang, C., Shi, Y., 2018. Potential enhancement of direct interspecies electron transfer for anaerobic degradation of coal gasification wastewater using up-flow anaerobic sludge blanket (UASB) with nitrogen doped sewage sludge carbon assisted. *Bioresour. Technol.* 270, 230–235.